

FOURTH ORDER TIME-STEPPING FOR LOW DISPERSION KORTEWEG-DE VRIES AND NONLINEAR SCHRÖDINGER EQUATIONS*

CHRISTIAN KLEIN[†]

Abstract. Purely dispersive equations, such as the Korteweg-de Vries and the nonlinear Schrödinger equations in the limit of small dispersion, have solutions to Cauchy problems with smooth initial data which develop a zone of rapid modulated oscillations in the region where the corresponding dispersionless equations have shocks or blow-up. Fourth order time-stepping in combination with spectral methods is beneficial to numerically resolve the steep gradients in the oscillatory region. We compare the performance of several fourth order methods for the Korteweg-de Vries and the focusing and defocusing nonlinear Schrödinger equations in the small dispersion limit: an exponential time-differencing fourth-order Runge-Kutta method as proposed by Cox and Matthews in the implementation by Kassam and Trefethen, integrating factors, time-splitting, Fornberg and Driscoll's 'sliders', and an ODE solver in MATLAB.

Key words. exponential time-differencing, Korteweg-de Vries equation, nonlinear Schrödinger equation, split step, integrating factor

AMS subject classifications. Primary, 65M70; Secondary, 65L05, 65M20

1. Introduction. The Korteweg-de Vries (KdV) equation,

$$(1.1) \quad u_t + \epsilon^2 u_{xxx} + 6uu_x = 0,$$

where $\epsilon > 0$ is a (small) scaling parameter describes one-dimensional wave phenomena in the limit of long wave lengths. It is well known that the corresponding dispersionless equation, the Hopf equation $u_t + 6uu_x = 0$ following from (1.1) for $\epsilon = 0$, develops for generic initial data a point of gradient catastrophe. The Burgers' equation, $u_t + 6uu_x = \epsilon u_{xx}$, can be seen as a dissipative regularization of the Hopf equation whose solutions tend for $\epsilon \rightarrow 0$ to the shock solution of the Hopf equation. The KdV equation provides a purely dispersive regularization of the Hopf equation, and its solutions develop a zone of rapid modulated oscillations in the shock region of the Hopf solution as can be seen in Fig. 1.1. Lax, Levermore [28], and Venakides [39] (see also [13]) gave an asymptotic description of these dispersive shocks. The asymptotic solution corresponding to the situation in Fig. 1.1 is shown there in green. The validity of this description was numerically studied in [17] in order to identify regions in the (x, t) -plane where the asymptotic description is not at least of order $\mathcal{O}(\epsilon)$.

The rigorous asymptotic description for KdV solutions in the low dispersion limit is based on the fact that the KdV equation is completely integrable, which implies the existence of powerful solution generating techniques. Another interesting equation in this context is the nonlinear Schrödinger (NLS) equation

$$(1.2) \quad i\epsilon u_t + \epsilon^2 u_{xx} - 2\sigma|u|^2 u = 0,$$

where $\sigma = -1$ in the focusing case and $\sigma = 1$ in defocusing case. It is again a purely dispersive completely integrable equation with important applications in nonlinear optics and hydrodynamics. Since the parameter ϵ takes the role of the \hbar in the usual Schrödinger equation, the low dispersion limit for the NLS equation is also referred to as its semiclassical limit. Lax-Levermore theory was extended to the defocusing case in [20]. In contrast to the KdV

*Received October 31, 2006. Accepted for publication December 14, 2007. Published online on May 21, 2008. Recommended by A. Frommer.

[†]Max Planck Institute for Mathematics in the Sciences, Inselstr. 22, 04103 Leipzig, Germany. Current address: Institut de Mathématiques de Bourgogne, Université de Bourgogne, 9 avenue Alain Savary, BP 47970 - 21078 Dijon Cedex, France (christian.klein@u-bourgogne.fr).

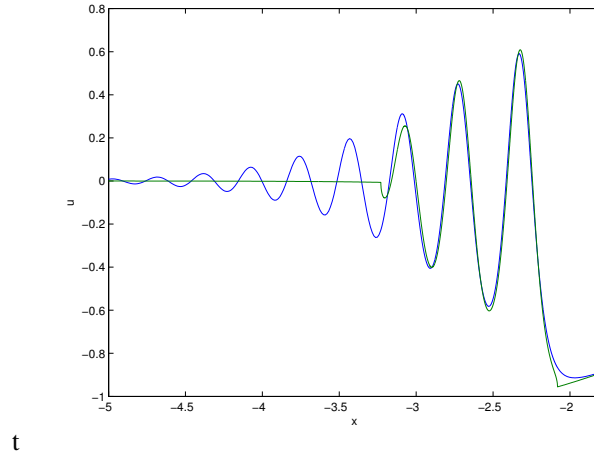


FIG. 1.1. The blue graph shows the solution to the KdV equation for $\epsilon = 0.1$ for the initial data $u_0(x) = -\text{sech}^2 x$ at the time $t = 0.4$, the green graph the corresponding asymptotic solution according to [28, 39, 13].

and the defocusing case, a comprehensive asymptotic description in the focusing NLS case exists only for special classes of initial data as given in [21] and [37]. Numerical studies of this limit have been presented in [8, 9, 10]. See [5, 6] for the use of exponential integrators for the NLS equations and [3, 4] for the use of time splitting to explore numerically the semiclassical limit of the defocusing NLS equation.

The numerical treatment of the low dispersion limit requires the resolution of a zone with rapid oscillations with strong gradients. Since the solutions for smooth initial data are known to be smooth for finite ϵ , spectral methods can be efficiently applied. We are studying here only Schwartzian initial data, which allows the use of Fourier methods. In Fourier space, equations (1.1) and (1.2) have the form

$$(1.3) \quad v_t = \mathbf{L}v + \mathbf{N}(v, t),$$

where v denotes the (discrete) Fourier transform of u , and where \mathbf{L} and \mathbf{N} denote linear and nonlinear operators, respectively. Equation (1.3) thus represents a system of ODEs after spatial discretization. The KdV and the NLS equations are classical examples of stiff equations, where the stiffness is related to the linear part \mathbf{L} (it is induced by the distribution of the eigenvalues of \mathbf{L}), whereas the nonlinear part has only low order derivatives. In the low dispersion limit, this stiffness is still present despite the small term ϵ^2 in \mathbf{L} . This is due to the fact that the smaller ϵ , the higher spatial frequencies are needed to resolve the rapid oscillations.

There are several approaches to deal efficiently with equations of the form (1.3) with a linear stiff part as implicit-explicit (IMEX), time splitting, integrating factor (IF), and deferred correction schemes as well as sliders and exponential time differencing. To avoid as much as possible a pollution of the Fourier coefficients by errors due to the finite difference schemes for the time integration and to allow for larger time steps, it is beneficial to consider fourth order schemes. In this paper we compare the performance of several fourth order schemes mainly related to exponential integrators for various examples in a similar way as in the work by Kassam and Trefethen [22].

The paper is organized as follows: In §2 we briefly list the used numerical schemes, integrating factor methods, exponential time differencing, Runge-Kutta sliders and time splitting methods. In §3 we study two examples for the KdV equation, the 2-soliton solution and a low

dispersion limit. In §4 a similar study is presented for the focusing and the defocusing NLS equation. The found numerical errors obtained are compared in §5 with the error indicated by a violation of energy conservation by the numerical solution. In §6 we consider potential stability problems in the numerical schemes for small ϵ , and in §7 we add some concluding remarks and outline further directions of research.

2. Numerical Methods. The numerical task in this paper consists in the solution of the KdV and the NLS equations in the limit of low dispersion for smooth Schwartzian initial data. The latter implies that we can treat the problem as essentially periodic and that we can use Fourier methods. After spatial discretization we thus face a system of ODEs of the form (1.3). Since we need to resolve high spatial frequencies, these systems will be in general rather large. In the present paper we have restricted the analysis to moderate values of the dispersion parameter ϵ to be able to compare different schemes in finite CPU time. For smaller values of ϵ ; see for instance [17].

We follow basically [22] in comparing several numerical schemes for equations of the form (1.3). We give the numerical error in dependence of the time step as well as the actual CPU time as measured by MATLAB (all computations are done on a G4 processor with 1.67GHz with MATLAB codes). Since MATLAB is using in general a mixture of interpreted and precompiled embedded code, a comparison of computing times is not unproblematic. However, it makes sense in the present context since the main computational cost in the compared numerical approaches (with the exception of the ODE solver ode15s considered only in one example) are in all cases 6 (embedded) FFT commands per time step as was already pointed out in [14]. The computation of the ϕ -functions in the ETD schemes is also done via FFT. The purpose of studying the computation time is to show that this implementation is very efficient and has only negligible effect on the total CPU time in the experiments. As the numerical error, we always consider the L_2 norm of the difference of the numerical solution and an exact or reference solution, normalized by the L_2 norm of the initial data. This error is denoted by Δ_2 . As in [22] we do not consider deferred correction [25] and exponential Runge-Kutta schemes of the type considered in [18].

Runge-Kutta sliders. The basic idea of IMEX methods (see e.g. [11]) for KdV is the use of an implicit and thus stable method for the linear part of the equation and an explicit scheme for the nonlinear part. In [22] these schemes did not perform satisfactorily in the considered cases, which is the reason why we ignore them here. Fornberg and Driscoll [16] gave an interesting generalization of this approach by splitting also the linear part of the equation in Fourier space in regimes of high, medium, and low frequencies, and to use different numerical schemes for the respective regimes. They considered the NLS equation as an example. Driscoll [14] has modified this idea in the form of an implicit-explicit third order Runge-Kutta scheme for the high frequencies and a standard fourth order Runge-Kutta scheme for the low frequencies. This is the method we will use here, denoted by RK slider. The scheme is applied in [14] also to a modified version of the NLS equation and to a 2 + 1-dimensional generalization of the KdV equation, the Kadomtsev-Petviashvili equation. Strictly speaking the scheme is only of third order for the high frequencies, but it was already observed in [14] that it performs actually like a fourth order method. We confirm this here for the cases where the method converges.

Splitting techniques. Split step methods seem to appear first in the work by Bagrinovskii and Godunov [1]; see [7, 35] for reviews. Yoshida [40] developed a method to generate split step schemes of arbitrary order by introducing fractional time steps. Splitting methods are especially effective if the equation splits into two equations, which can be directly integrated. This is the case for the NLS equation, which can be split into

$$i\epsilon u_t = -2\epsilon^2 u_{xx},$$

$$i\epsilon u_t = 4\sigma|u|^2u.$$

The first equation can be explicitly integrated in Fourier space. The second equation has the property that $|u|^2$ is time independent. It can thus be explicitly integrated in physical space. The only error in the scheme in addition to the discretization error is thus due to the splitting. We use fourth order splitting as in [16] and [1] for the NLS equation.

A similar way to split KdV would be a splitting into a linear equation and the Hopf equation

$$\begin{aligned} u_t &= -2\epsilon^2 u_{xxx}, \\ u_t &= -12uu_x. \end{aligned}$$

Whereas the first equation can be again explicitly integrated in Fourier space, the Hopf equation can be integrated only implicitly with the method of characteristics, $u(t, x) = u_0(\xi)$, where $u_0(x)$ are the initial data and where ξ satisfies $x = 12u_0(\xi)t + \xi$. The latter relation can be solved iteratively which is, however, numerically expensive, especially since the function u from the last time step, which is used as initial data for the current step, needs to be evaluated at intermediate points. This implies the use of some interpolation. In [22] the Hopf equation was consequently solved with a fourth order Runge-Kutta scheme which was, however, not efficient. Therefore we use time splitting only for the NLS equation.

Integrating Factor (IF). Integrating factor methods appeared first in the work of Lawson [27]; see [31] for a comprehensive review. The basic idea is to use an integrating factor for the equation (1.3) and to rewrite it as

$$(e^{L_t}v)_t = e^{L_t}\mathbf{N}(u, t),$$

and then to use an explicit method for the time integration of the new dependent variable $e^{L_t}v$. We use here a standard fourth order Runge-Kutta scheme. Hochbruck and Ostermann [19] showed that this method only is of first order for semilinear parabolic problems in the ‘stiff’ regime, but of fourth order in the ‘non-stiff’ regime. Up to now there is no extension of this theory to hyperbolic equations, but the results in [6] for the defocusing NLS equation indicate that similar behavior is to be expected for hyperbolic equations (both KdV and NLS are hyperbolic).

Exponential time differencing (ETD). Exponential time differencing schemes are known for a long time in computational electrodynamics; see [31] for a comprehensive review of ETD methods and their history. The basic idea is to use equidistant time steps h and to integrate equation (1.3) exactly between the time steps t_n and t_{n+1} with respect to t . With $v(t_n) = v_n$ and $v(t_{n+1}) = v_{n+1}$, we get

$$v_{n+1} = e^{Lh}v_n + \int_0^h d\tau e^{L(h-\tau)}\mathbf{N}(v(t_n + \tau), t_n + \tau),$$

and to compute the integral in an approximate way. We use here the Runge-Kutta scheme by Cox and Matthews [12]. Hochbruck and Ostermann [19] showed that this scheme is only of second order in the ‘stiff’ regime of the equation, but of fourth order in the ‘non-stiff’ regime. There are fourth order ETD schemes which are also of fourth order in the stiff regime as the one given in [26, 19]; see also [31]. All these methods show the same performance in the non-stiff regime. Since we find that the Cox-Matthews method is of fourth order for the examples we consider here, we only apply this method as a typical representative for ETD.

The main numerical problem with ETD schemes is the efficient and accurate numerical evaluation of the functions

$$\phi_i(z) = \frac{1}{(i-1)!} \int_0^1 e^{(1-\tau)z} \tau^{i-1}, \quad i = 1, 2, 3, 4,$$

i.e., functions of the form $(e^z - 1)/z$, where one has to avoid cancellation errors. Kassam and Trefethen [22] used complex contour integrals to compute these functions. The approach is straight forward for diagonal operators \mathbf{L} that occur here: one considers a unit circle around each point z and computes the contour integral with the trapezoid rule. Schmelzer [36] recently made this approach more efficient by using the complex contour approach only for values of z close to the pole, e.g., with $|z| < 1/2$. For the same values of z the functions ϕ_i can be computed via a Taylor series. These two independent and very efficient approaches allow a control of the accuracy. We find that just 16 Fourier modes in the computation of the complex contour integral are sufficient to determine the functions ϕ_i to the order of machine precision. For the 1 + 1-dimensional equations we consider here, this computation takes only negligible time, especially since it has to be done only once during the time evolution. We find that ETD as implemented in this way has the same computational costs as the other used schemes. As already mentioned, these costs are essentially given by the number of FFT evaluations at each time step, which is 6 for all of the above methods.

ODE solver in MATLAB. MATLAB is distributed with a collection of ODE solvers, see [33, 34], which are designed for a wide range of ODE problems. For stiff ODE systems, such as (1.3), ode15s is the recommended solver if one is interested in more than low accuracy. For the examples studied in this paper, ode15s generally performs poorly and is never close to competitive to the above listed methods. We could only perform more systematic tests for the system of smallest size, the KdV 2-soliton example with 512 modes. For larger systems, ode15s simply took too much computing time despite the use of an analytic Jacobian.

3. Korteweg-de Vries equation. Since the KdV equation is completely integrable, large classes of exact solutions are explicitly known, the most prominent being the solitonic solutions. Before addressing the low dispersion limit, we will first reproduce the 2-soliton solution used as a test case in [22] for ease of reference. We will consider exponential time differencing, Runge-Kutta sliders, and an integrating factor method for KdV.

3.1. 2-soliton solution. In [22] initial data of the form

$$u(x, 0) = \frac{A^2}{2} \operatorname{sech}^2 \left(\frac{A(x+2)}{2} \right) + \frac{B^2}{2} \operatorname{sech}^2 \left(\frac{B(x+1)}{2} \right)$$

were considered for $A = 25$, $B = 16$, and $\epsilon = 1$ (notice the different normalization of u here).

The results for a simulation with $t \leq 0.001$ for $N = 512$ modes are presented in Fig. 3.1. The data are fitted with straight lines via linear regression analysis in a doubly logarithmic plot, $\log_{10} \Delta_2 = -a \log_{10} N_t + b$. We find $a = 4.8$ for RK sliders, $a = 4.3$ for the integrating factor method and for ETD.

It can be seen that all methods show fourth order convergence. Thus there is no Hochbruck-Ostermann transition [19] in this example from a stiff to a non-stiff region. The RK slider method performs best, followed by the ETD and the IF method. The same holds, if one considers the dependence of the numerical error on CPU time as can be seen in Fig. 3.1. Thus the computation of the ϕ functions for the ETD scheme has already here no noticeable effect on the computing time.

The 2-soliton example was the only one where we could perform more systematic tests with the MATLAB ODE solver ode15s. We called the solver with different values of the desired relative and absolute accuracy. Without an restriction of the used order of the method, ode15s failed to converge consistently for higher resolutions, for which the problem is stiffer. If the maximal order of the scheme is set to be equal to 2, ode15s always converges. This

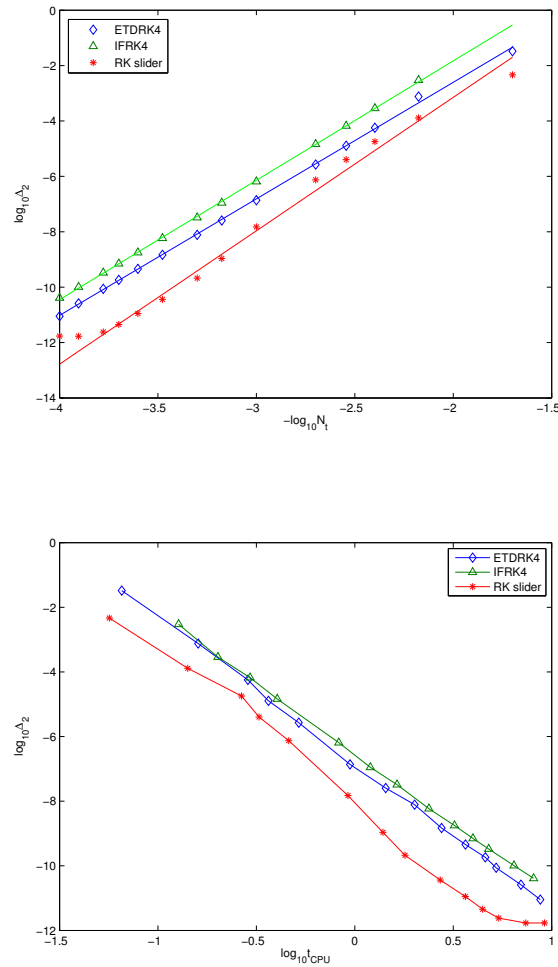


FIG. 3.1. Normalized L_2 norm of the numerical error for several numerical methods, as a function of N_t (top) and as a function of CPU time (bottom). The shown straight lines have slopes 4.8 for RK sliders, 4.3 for the integrating factor method and for ETD.

seems to reflect the second Dahlquist barrier for hyperbolic systems: ode15s appears to be unstable for stiff problems of the considered type if it uses higher order approaches. We show in Fig. 3.2 the error Δ_2 in dependence of the time steps used by ode15s and the computing time. Even at low accuracies, ode15s cannot compete with the other numerical methods, which is why we presented it in a separate plot. The error for ode15s for a prescribed relative tolerance of 10^{-2} and below shows the expected second order behavior for the fixed maximal order.

3.2. Small dispersion limit. This result for the performance of the numerical methods known from [22] changes considerably when we consider a typical example for an initial value problem for low dispersion KdV. As in [17] we consider initial data $u_0 = -\text{sech}^2 x$ for $\epsilon = 0.1$. It can be seen in Fig. 3.3 that at time $t_c \sim 0.2$ an oscillatory region with strong

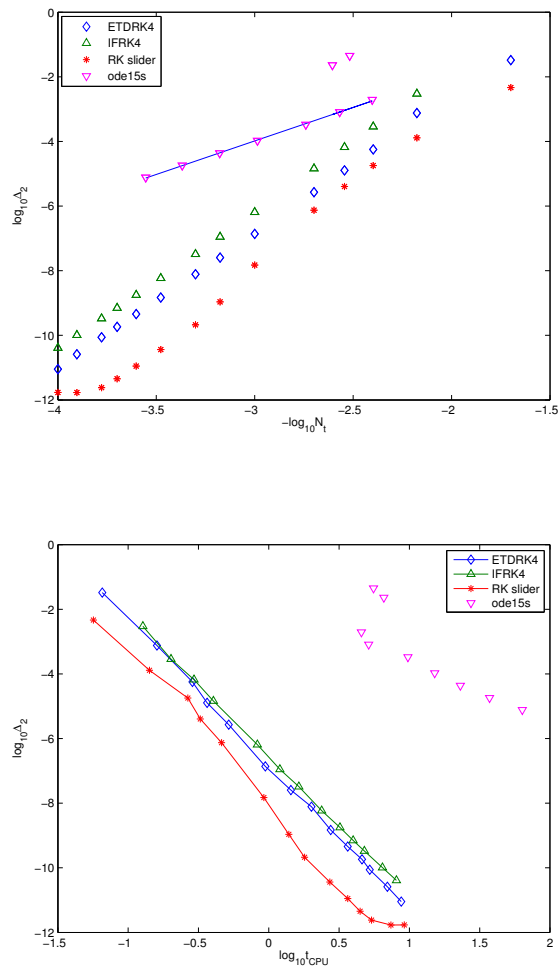


FIG. 3.2. Normalized L_2 norm of the numerical error for several numerical methods, as a function of N_t (top) and as a function of CPU time (bottom). The shown line has slope 2.08.

gradients appears. The resolution of these oscillations requires high spatial frequencies and thus leads to a rather stiff term in the equation via the third derivative in (1.1), though this term is multiplied by the small quantity ϵ^2 .

The computations are carried out on a grid for $x \in [-5\pi, 5\pi]$ with 2^{11} points. With this resolution, the spectral coefficients at time 0.4 go down to 10^{-12} ; see Fig. 6.1. As a reference solution we consider the arithmetic mean of the solutions obtained with the considered numerical methods for $N_t = 20000$ time steps. The dependence of the normalized L_2 norm of the difference between this reference solution and the numerical solution is shown in Fig. 3.4.

It can be seen that the RK slider method converges in this case only for very small time steps, where the numerical error is already of the order of 10^{-5} . This is in remarkable contrast to the above soliton example. ETD is the most efficient and the most robust method in this

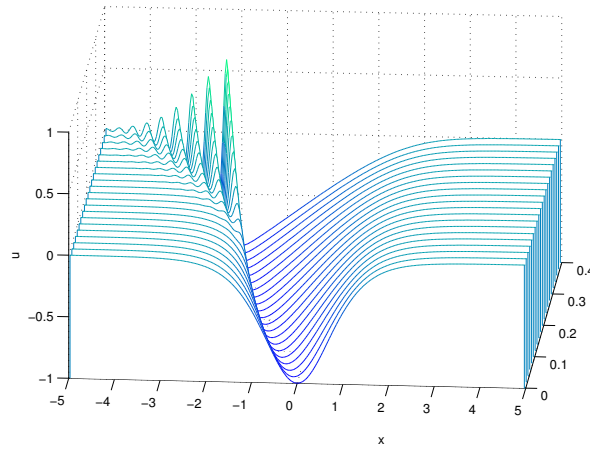


FIG. 3.3. Solution to the KdV equation with $\epsilon = 0.1$ for the initial data $u_0 = -\text{sech}^2 x$.

case, since it converges also for comparatively large time steps. Due to the large number of time steps necessary in this example, the computation of the ϕ -functions in the ETD scheme has no noticeable effect as can be seen from the dependence of the numerical error on CPU time in Fig. 3.4. For comparatively large time steps, all schemes seem to perform slightly worse than 4th order, but a clear transition between a stiff and a non-stiff region as in [19] cannot be identified. A linear regression analysis of the whole ETD data in Fig. 3.4 as for the soliton example above leads to an exponent of 3.9. Thus the schemes show fourth order convergence for this example as well, and ETD performs best in this context.

4. Nonlinear Schrödinger equation. The focusing and defocusing NLS equation show considerably different behavior in many respects, where the defocusing version is rather close to the KdV equation. We study examples for both versions.

4.1. Breather solution. The focusing NLS equation has solitonic solutions with zero speed, which lead to pulsating solutions, so-called breathers. These solutions were used in [30, 21, 29] as a setting to study the low dispersion limit of the focusing NLS equation. As was shown in [32], they lead to initial data of the form $u_0 = M \text{sech}(x)$, where M is an integer. The simplest breather solution has the form

$$u = 4 \exp(it) \frac{\cosh(3x) + 3 \exp(8it) \cosh(x)}{\cosh(4x) + 4 \cosh(2x) + 3 \cos(8t)}.$$

The solution is periodic in time with period 2π . In Fig. 4.1 we show the square of the absolute value for this solution for $t \leq \pi/4$. One can see the typical focusing behavior of solutions to the focusing NLS, which leads to a blow up of the derivatives of the solutions to the dispersionless equation. Thus the breather already offers a good test case for the semiclassical limit.

The computation is carried out with 2^{11} points for $x \in [-10\pi, 10\pi]$. The numerical error is shown in Fig. 4.2. All numerical schemes show a clear fourth order behavior as can be seen from the straight lines in a doubly logarithmic plot with slope $a = 4.0$ for RK sliders, $a = 3.5$ for the split step method, $a = 3.9$ for the integrating factor method, and $a = 4.1$ for ETD. The split step method shows fourth order behavior, but reaches its maximal precision at roughly $10^{-7.5}$. This appears to be due to a resonance between numerical errors in the two equations

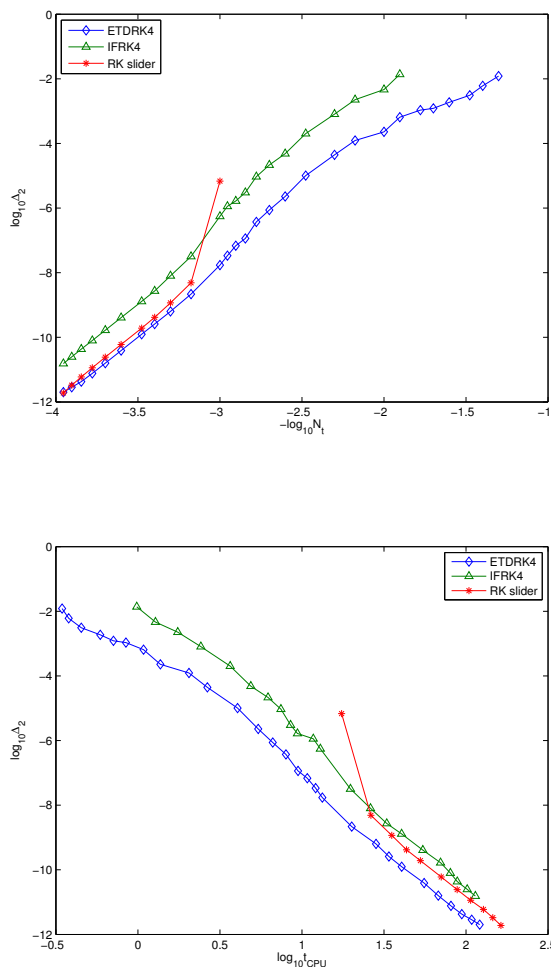


FIG. 3.4. Normalized L_2 norm of the numerical error for several numerical methods, as a function of N_t (top) and as a function of CPU time (bottom).

into which NLS is split in this approach. This resonance seems to impose a limit on the maximal achievable accuracy by this approach. However, this is without practical relevance, since normally solutions are not needed with such a high precision. In this example, the RK slider method is the most efficient one followed by ETD, IF and the splitting methods.

4.2. Semiclassical limit for the focusing NLS. To study the semiclassical limit of the focusing NLS equation, we consider initial data of the form $u_0 = \exp(-x^2)$ for $\epsilon = 0.1$. As can be seen in Fig. 4.3, the square of the absolute value of u for the initial pulse is focused until it reaches maximal height at time $t \sim 0.26$, where the strongest gradient appears. After this time the plot shows several smaller humps of similar shape as the one at breakup of the dispersionless equation.

The computation is carried out with 2^{13} points for $x \in [-5\pi, 5\pi]$. Again the splitting method allows for a maximal precision of 10^{-8} . To determine a reference solution, we com-

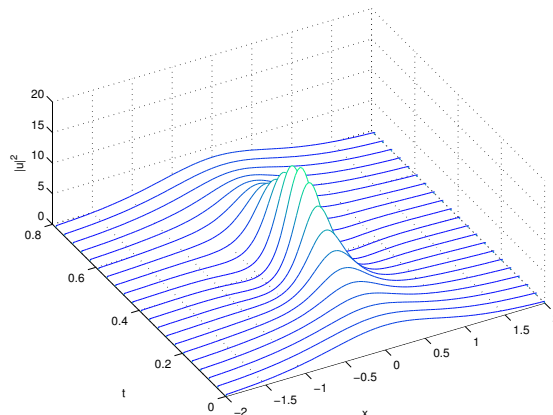


FIG. 4.1. *Breather solution for the focusing NLS equation.*

pute solutions with 20000 time steps with the ETD, the RK slider and the IF schemes and take the arithmetic mean. The normalized L_2 norm of the difference of the numerical solutions with respect to this reference solution is shown in Fig. 4.4. All schemes show fourth order convergence as can be seen from the straight lines with slope $a = 4.1$ for RK sliders, $a = 3.8$ for the split step method, $a = 3.9$ for the integrating factor method, and $a = 4.2$ for ETD. The performance of the numerical methods is as in the breather case above, RK slider being the most efficient.

4.3. Semiclassical limit for the defocusing NLS. To study the semiclassical limit of the defocusing NLS equation, we consider as in the focusing case initial data of the form $u_0 = \exp(-x^2)$ for $\epsilon = 0.1$. As can be seen in Fig. 4.5 for the square of the absolute value of u , the behavior of the solution is quite different from the focusing case and much closer to the KdV situation. The initial pulse is broadened but gets steeper on both sides. Before reaching the point of gradient catastrophe, oscillations appear which are in the considered example, however, quite small.

Since the gradients are comparatively small in this example, spectral resolution is achieved with 2^{10} points. Again the splitting method reaches a maximal precision of the order of 10^{-8} . Thus we take the arithmetic mean of the solutions for RK slider, ETD and IF with 20000 time steps as the reference solution. It can be seen from Fig. 4.6 that in contrast to the focusing case, the splitting method is by far the most efficient. The RK slider, ETD and IF methods almost perform identically. All methods show fourth order convergence as can be seen from the straight line with slope $a = 4.0$. In the defocusing case the efficiency of the shown numerical methods is almost reversed with respect to the focusing case. The splitting method clearly outperforms the other methods both in terms of time steps and CPU time.

5. Conservation Laws. The KdV and NLS equations belong to the family of completely integrable equations which means they have an infinite number of conserved quantities, the most well known being mass, energy and momentum. The unavoidable numerical error during the time evolution implies that these conserved quantities are numerically not conserved unless their conservation is implemented in the code. Thus, the check to which extent a conserved quantity of the respective equation is also numerically conserved could provide some control of the quality of the numerical scheme in a specific case. This is espe-

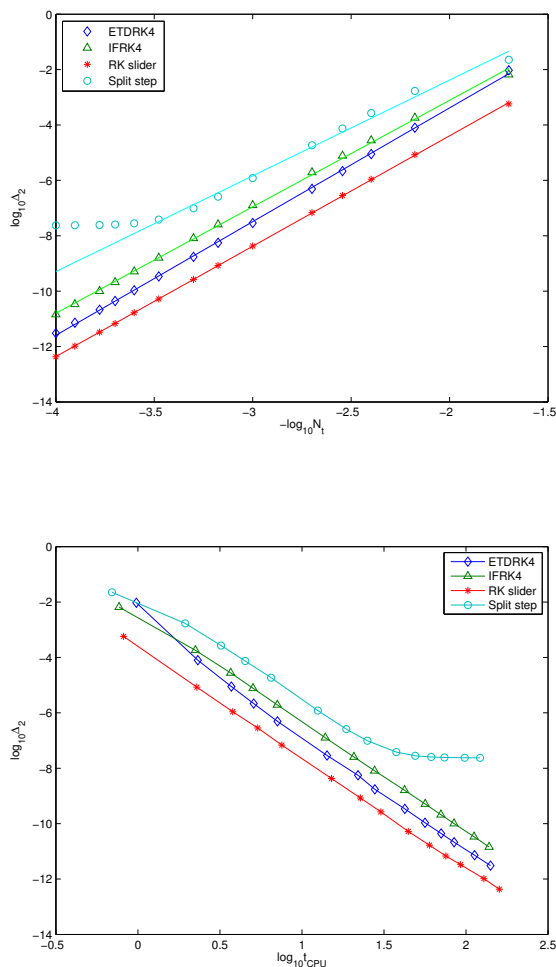


FIG. 4.2. Normalized L_2 norm of the numerical error for several numerical methods, as a function of N_t (top) and as a function of CPU time (bottom). The shown straight lines have slope 4.0 for RK sliders, 3.5 for split step, 3.9 for the integrating factor method, and 4.1 for ETD.

cially true in the here studied low dispersion limit, where one typically would like to explore also the cases, which are at the memory limits of the used computer. In these cases, the approach used in the previous sections to compare a solution with one obtained with the same scheme but at higher resolution is not easily available.

Most of the conserved quantities involve high order derivatives, which would be difficult to resolve numerically in a satisfactory way even with spectral methods. We will thus only consider conserved quantities, which contain at most first derivatives. A convenient choice is the energy, which for KdV takes the form (up to an unimportant multiplicative constant)

$$(5.1) \quad E = 2u^3 - \epsilon^2 u_x^2,$$

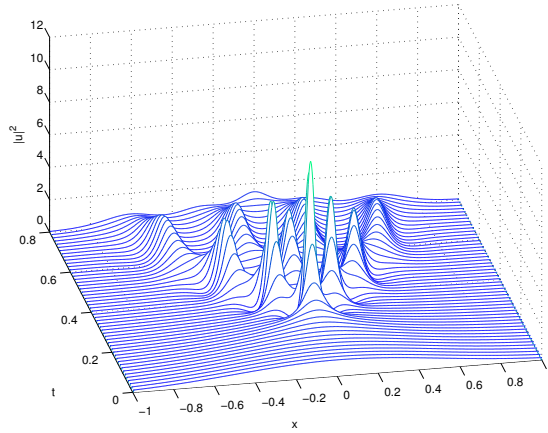


FIG. 4.3. Solution to the focusing NLS with $\epsilon = 0.1$ for the initial data $u_0 = \exp(-x^2)$.

and for NLS

$$(5.2) \quad E = \epsilon^2 |u_x|^2 + \sigma |u|^4.$$

Numerically the energy E is a function of time. We define $\Delta E := |(E(t) - E(0))/E(0)|$ and show the resulting error for the previously studied low dispersion examples. Typically one is interested in solutions to the PDEs considered here to an accuracy between 10^{-3} to 10^{-6} , i.e., the numerical error should be smaller than ϵ , since the asymptotic solution provides a description with an error up to order ϵ . Thus, the question is whether energy conservation provides a useful criterion in this range of the numerical precision.

In Fig. 5.1 the dependence of ΔE on the time step is shown for the KdV example of Fig. 3.4. Since the RK slider method only performed well in this example for accuracies below 10^{-8} , it is not surprising that energy conservation does not provide a valid criterion for numerical precision in this case. For IF and ETD, a comparison with Fig. 3.4 shows that energy conservation overestimates the numerical precision by a factor of 50 respectively 30, i.e., roughly by one to two orders of magnitude. It is interesting to note that the quantity ΔE decreases by roughly an order of magnitude faster with the time step than the error Δ_2 defined via the L_2 norm, i.e., it decreases roughly like 5th order where the scheme shows fourth order convergence as can be seen from the straight line in Fig. 5.1 with slope 4.7. This higher order convergence, which will be observed also for the focusing NLS, appears to be due to the fact that the terms leading to a fourth order error have divergence structure and thus do not contribute to the integrals (5.1) and (5.2).

The corresponding error in energy conservation for the low dispersion focusing NLS example of Fig. 4.4 is shown in Fig. 5.2. The error in the RK slider case can be fitted with a straight line with slope 5.1. Thus one obtains again fifth order convergence in this case. Because of this rapid decrease with the time step, the numerical error Δ_2 in the range between 10^{-3} and 10^{-6} overestimates the actual accuracy by up to 3 orders of magnitude for IF, ETD and RK slider. It is more or less useless for the splitting method.

The example for the low dispersion defocusing NLS of Fig. 4.6 is shown in Fig. 5.3. Similarly as for the L_2 error, the IF, ETD and RK slider methods perform almost identically with respect to the error in energy conservation. The error shows a fourth order behavior here, the shown straight line has a slope of 4.0. The numerical error Δ_2 in the range between 10^{-3}

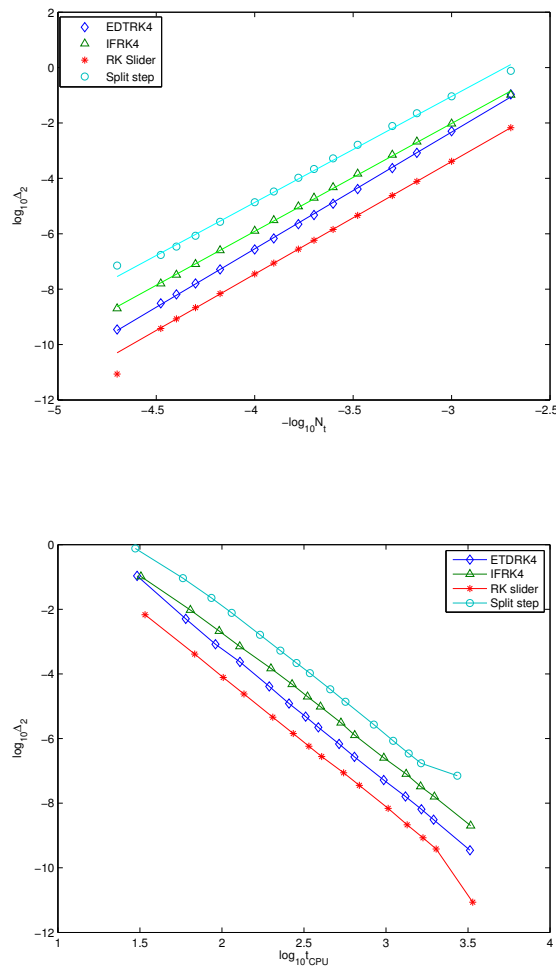


FIG. 4.4. Normalized L_2 norm of the numerical error for several numerical methods, as a function of N_t (top) and as a function of CPU time (bottom). The shown straight lines have slope 4.1 for RK sliders, 3.8 for split step, 3.9, for the integrating factor method, and 4.2 for ETD.

and 10^{-6} is almost identical to the one indicated by the violation of energy conservation.

The above examples show that energy conservation can be a useful indicator of the numerical accuracy, but it has to be used with care. Due to a fifth order dependence on the time step for the KdV and the focusing NLS examples, the numerical accuracy is overestimated in the range of interest by 2 respectively 3 orders of magnitude. For defocusing NLS, the numerical error indicated by energy conservation is almost identical to the error obtained from the L_2 norm of the difference between the numerical and a reference solution.

6. High spatial frequencies. One reason to use fourth order time stepping schemes in the numerical exploration of the low dispersion limit of dissipationless equations is to avoid as much as possible a pollution of the high spatial frequencies due to numerical errors caused by the finite difference time integration. Resulting numerical errors can lead, e.g., to

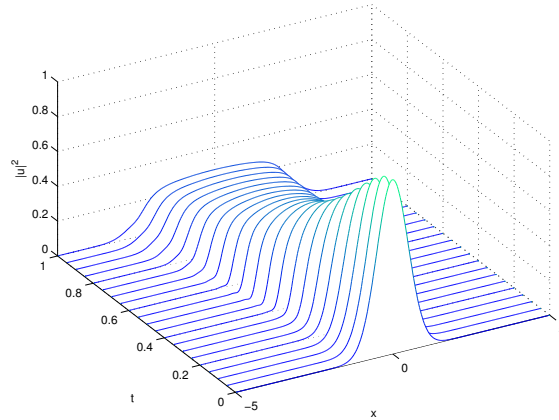


FIG. 4.5. Solution to the defocusing NLS with $\epsilon = 0.1$ for the initial data $u_0 = \exp(-x^2)$.

aliasing errors in the Fourier approach since we are considering nonlinear equations. Such errors typically show up in the Fourier coefficients for the high spatial frequencies, which should decrease exponentially with the frequency for smooth functions. In fact, we find this behavior for all studied examples as long as we use sufficient spatial resolution, i.e., as long as the Fourier coefficients of the highest spatial frequencies go down to the order of machine precision for the considered solution in the entire range of t . Since all schemes perform very similarly in this context, we show here only plots for ETD.

For the KdV example the exponential decrease of the Fourier coefficients with k can be seen clearly in Fig. 6.1. In practice, however, it will not always be possible to provide a spatial resolution of the order of machine precision to avoid high frequency problems. Moreover, this would not be economical if one wants to explore the low dispersion limit for small values of ϵ . In the second figure in Fig. 6.1, the same qualitative behavior of the Fourier coefficients is observed even if the resolution is considerably reduced.

The situation is very similar in the case of the defocusing NLS equation. However, resolution problems show up in the case of the focusing NLS equation as can be seen in Fig. 6.2 for the breather solution in two resolutions.

The second plot in Fig. 6.2 shows that 2^{10} points would in principle be enough to spatially resolve the shown end state to the order of machine precision. This is, however, not the case for the highly focused pulse at time $t = \pi/8$. This lack of resolution (see Fig. 6.3) leads to the problems in the high spatial frequencies at time $t = \pi/4$ visible in Fig. 6.2.

Since the breather solution already shows the main features of a generic solution to the focusing NLS equation in the semiclassical limit for analytic initial data, we just mention that the same problems also appear there. In all these cases maximal spatial resolution is needed to resolve the pulse at break-up. The reason for the different behavior in the different cases is the following: For the KdV and defocusing NLS equations, the dispersionless limit leads again to a hyperbolic equation. For the focusing NLS equation, the semiclassical limit leads to an elliptic system, which is the reason for the so called modulation instability, see, e.g., [15] and references therein. In the latter case, unavoidable numerical errors due to finite precision computation lead to growing unstable modes showing up in the form of Fourier coefficients for the high spatial frequencies strongly growing with time as discussed by Krasny [24] in a similar context. To avoid numerical instabilities, Krasny filtering (coefficients of absolute

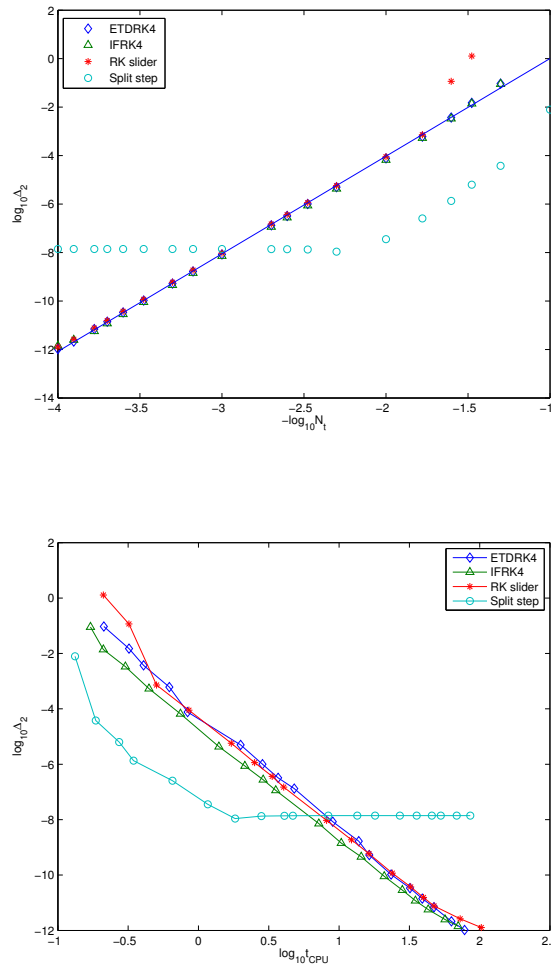


FIG. 4.6. Normalized L_2 norm of the numerical error for several numerical methods, as a function of N_t (top) and as a function of CPU time (bottom). The shown straight line has slope 4.0.

value below a certain threshold, e.g., 10^{-12} are set to zero) or the use of higher precision computation is necessary.

7. Conclusion. In this paper we have shown that fourth order time stepping schemes can be efficiently used to study numerically the low dispersion limit for the KdV and NLS equations. All codes showed fourth order convergence, but with considerably different performance in different cases, which makes clear that the best choice of the method depends on the specific problem. In the present case, ETD was most efficient for KdV, RK slider for the focusing NLS, and splitting for the defocusing NLS. Stability problems due to the lack of spatial resolution only occurred in the focusing NLS case.

The used methods also can be applied to study similar low dispersion limits for 2 + 1-dimensional system as the Kadomtsev–Petviashvili and the Davey–Stewartson equation in [23]. Since for 2 + 1-dimensional cases no asymptotic description has been given, numeri-

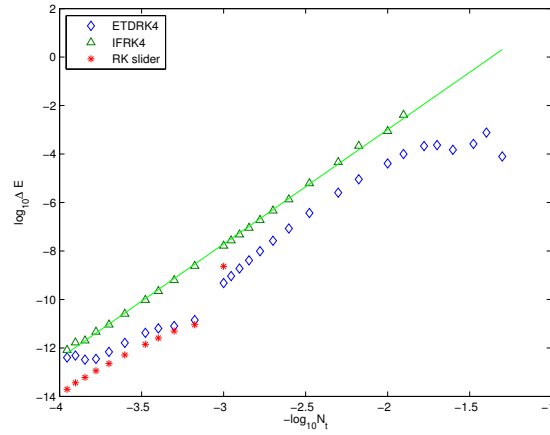


FIG. 5.1. Normalized violation of energy conservation for the KdV solution with initial data $u_0 = -\text{sech}^2 x$ and $\epsilon = 0.1$ for several numerical methods. The shown straight line has slope 4.7.

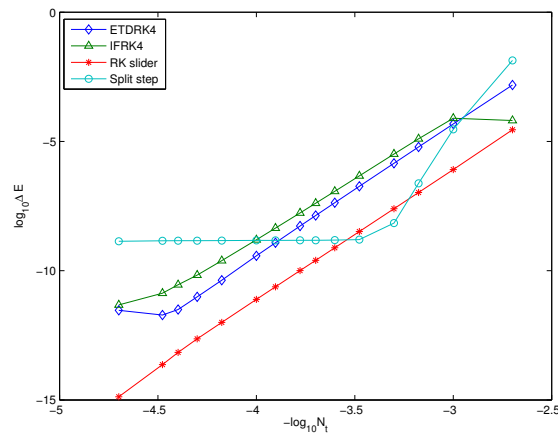


FIG. 5.2. Normalized violation of energy conservation for the focusing NLS solution with initial data $u_0 = \exp(-x^2)$ and $\epsilon = 0.1$ for several numerical methods. The shown straight line has slope 5.1.

cal approaches are very instructive to gain analytic insight. A systematic study of fourth order numerical approaches in this context is in progress.

Acknowledgments. The author thanks W. Bao, B. Dubrovin, J. Frauendiener, T. Grava, P. Markowich, P. Matthews, and A. Ostermann for helpful discussions and hints. Special thanks go to T. Schmelzer and L. N. Trefethen, who interested him in exponential integrators, for providing codes and invaluable information. The work was supported in part by MISGAM program of the European Science Foundation.

REFERENCES

- [1] K. A. BAGRINOVSKII AND S. K. GODUNOV, *Difference schemes for multi-dimensional problems*, Dokl.

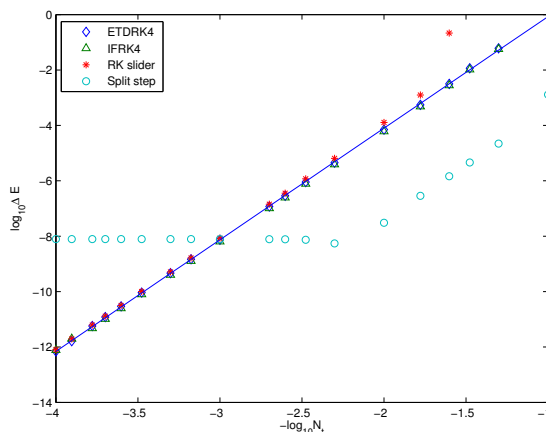


FIG. 5.3. Normalized violation of energy conservation for the defocusing NLS solution with initial data $u_0 = \exp(-x^2)$ and $\epsilon = 0.1$ for several numerical methods. The shown straight line has a slope of 4.0.

- Acad. Nauk, 115 (1957), pp. 431–433.
- [2] W. BAO AND Y. ZHANG, *Dynamics of the ground state and the central vortex states in Bose-Einstein condensation*, Math. Mod. Meth. Appl. Sci., 15 (2005), pp. 1863–1896.
 - [3] W. BAO, S. JIN, AND P. A. MARKOWICH, *On time-splitting spectral approximations for the Schrödinger equation in the semiclassical regime*, J. Comput. Phys., 175 (2002), pp. 487–524.
 - [4] W. BAO, S. JIN, AND P. A. MARKOWICH, *Numerical study of time-splitting spectral discretizations of nonlinear Schrödinger equations in the semi-classical regimes*, SIAM J. Sci. Comp., 25 (2003), pp. 27–64.
 - [5] H. BERLAND, A. L. ISLAS, AND C. M. SCHÖBER, *Solving the nonlinear Schrödinger equation using exponential integrators*, J. Comput. Phys., 255 (2007), pp. 284–299.
 - [6] H. BERLAND AND B. SKAFLESTAD, *Conservation of phase space properties using exponential integrators on the cubic Schrödinger equation*, in Proceedings of the 46th SIMS Conference on Simulation and Modeling, 2005, Trondheim, Norway, pp. 9–18. Available at <http://www.math.ntnu.no/preprint/>.
 - [7] J. P. BOYD, *Chebyshev and Fourier Spectral Methods*, Dover, Mineola, NY, 2001. Available at <http://www-personal.engin.umich.edu/~jpbayd/>.
 - [8] J. C. BRONSKI AND J. N. KUTZ, *Numerical simulation of the semi-classical limit of the focusing nonlinear Schrödinger equation*, Phys. Lett. A, 254 (1999), pp. 325–336.
 - [9] H. D. CENICEROS, *A semi-implicit moving mesh method for the focusing nonlinear Schrödinger equation*, Comm. Pure Appl. Anal., 1 (2002), pp. 1–18.
 - [10] H. D. CENICEROS AND FEI-RAN TIAN, *A numerical study of the semi-classical limit of the focusing nonlinear Schrödinger equation*, Physics Lett A, 306 (2002), pp. 25–34.
 - [11] T. F. CHAN AND T. KERKHOVEN, *Fourier methods with extended stability intervals for the Korteweg de Vries equation*, SIAM J. Numer. Anal., 22 (1985), pp. 441–454.
 - [12] S. M. COX AND P. C. MATTHEWS, *Exponential time differencing for stiff systems*, J. Comput. Phys., 176 (2002), pp. 430–455.
 - [13] P. DEIFT, S. VENAKIDES, AND X. ZHOU, *New result in small dispersion KdV by an extension of the steepest descent method for Riemann-Hilbert problems*, Internat. Math. Res. Notices, 6 (1997), pp. 286–299.
 - [14] T. A. DRISCOLL, *A composite Runge-Kutta method for the spectral solution of semilinear PDEs*, J. Comput. Phys., 182 (2002), pp. 357–367.
 - [15] B. DUBROVIN, T. GRAVA, AND C. KLEIN, *On universality of critical behaviour in the focusing nonlinear Schrödinger equation, elliptic umbilic catastrophe and the tritonquée solution to the Painlevé-I equation*, J. Nonlinear Sci., to appear.
 - [16] B. FORNBERG AND T. A. DRISCOLL, *A fast spectral algorithm for nonlinear wave equations with linear dispersion*, J. Comput. Phys., 155 (1999), pp. 456–467.
 - [17] T. GRAVA AND C. KLEIN, *Numerical solution of the small dispersion limit of Korteweg de Vries and Whitham equations*, Comm. Pure Appl. Math., 60 (2007), pp. 1623–1664.
 - [18] M. HOCHBRUCK, C. LUBICH, AND H. SELHOFER, *Exponential integrators for large systems of differential equations*, SIAM J. Sci. Comput., 19 (1998), pp. 1552–1574.

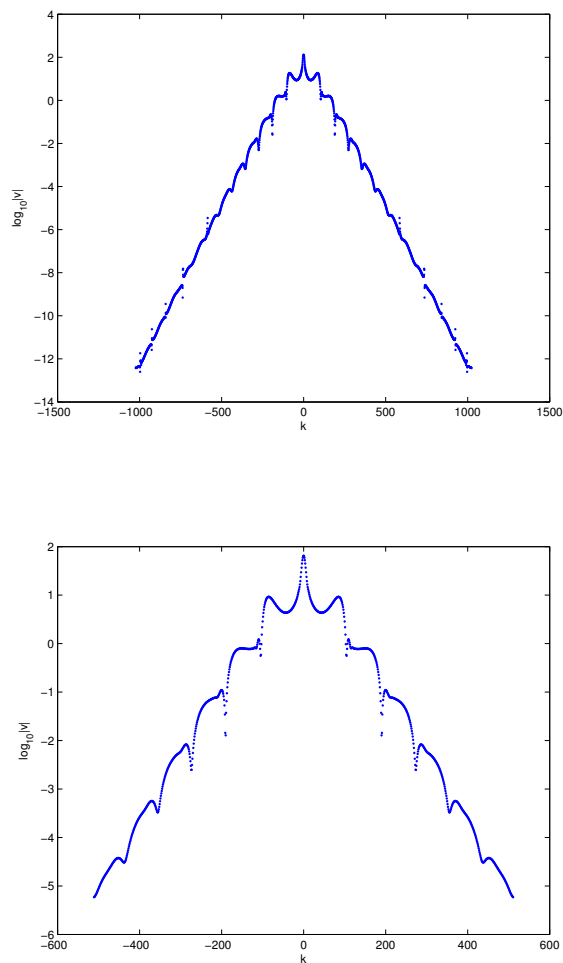


FIG. 6.1. Solution to the KdV equation with $\epsilon = 0.1$ for the initial data $u_0 = -\text{sech}^2 x$ at $t = 0.4$. The plots show the Fourier coefficients v in dependence of the spatial frequencies k for 2^{11} (top) and 2^{10} (bottom) points.

[19] M. HOCHBRUCK AND A. OSTERMANN, *Exponential Runge-Kutta methods for semilinear parabolic problems*, SIAM J. Numer. Anal., 43 (2005), pp. 1069–1090.

[20] S. JIN, D. D. LEVERMORE, AND D. W. MCLAUGHLIN, *The semiclassical limit of the Defocusing NLS Hierarchy*, Comm. Pure Appl. Math., 52 (1999), pp. 613–654.

[21] S. KAMVISSIS, K. D. T.-R. MCLAUGHLIN, AND P. D. MILLER, *Semiclassical Soliton Ensembles for the Focusing Nonlinear Schrödinger Equation*, Annals of Mathematics Studies, 154, Princeton University Press, Princeton, NJ, 2003.

[22] A.-K. KASSAM AND L. N. TREFETHEN, *Fourth-order time-stepping for stiff PDEs*, SIAM J. Sci. Comput., 26 (2005), pp. 1214–1233.

[23] C. KLEIN, C. SPARBER, AND P. MARKOWICH, *Numerical Study of oscillatory regimes in the Kadomtsev-Petviashvili equation*, J. Nonlinear Sci., 17 (2007), pp. 429–470.

[24] R. KRASNY, *A study of singularity formation in a vortex sheet by the point-vortex approximation*, J. Fluid Mech., 167 (1986), pp. 65–93.

[25] W. KRESS AND B. GUSTAFSSON, *Deferred correction methods for initial value boundary problems*, SIAM J. Sci. Comput., 17 (2002), pp. 241–251.

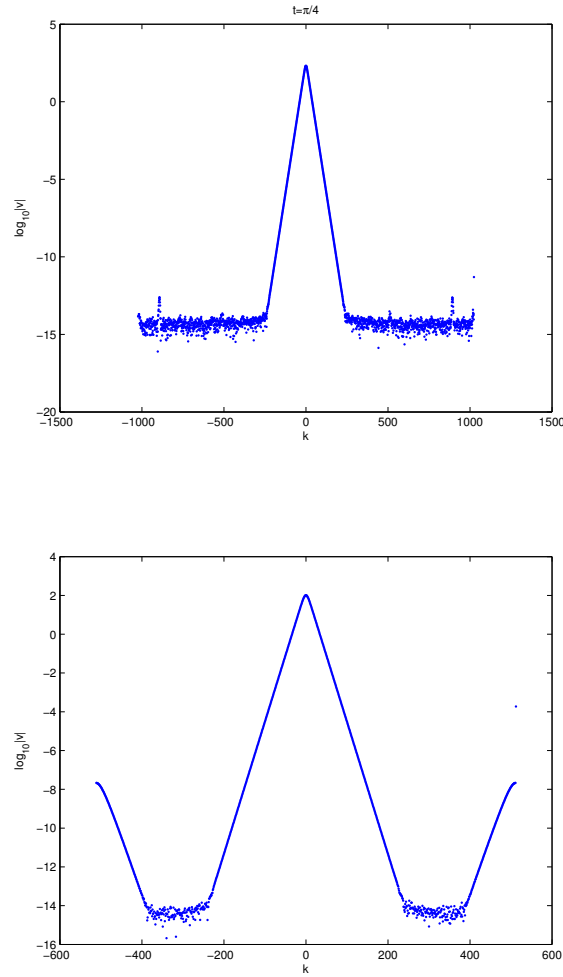


FIG. 6.2. Breather solution to the focusing NLS equation at $t = \pi/4$. The plots show the Fourier coefficients v in dependence of the spatial frequencies k for 2^{11} (top) and 2^{10} (bottom) points.

- [26] S. KROGSTAD, *Generalized integrating factor methods for stiff PDEs*, J. Comput. Phys., 203 (2005), pp. 72–88.
- [27] J. D. LAWSON, *Generalized Runge-Kutta processes for stable systems with large Lipschitz constants*, SIAM J. Numer. Anal., 4 (1967), pp. 372–380.
- [28] P. D. LAX AND C. D. LEVERMORE, *The small dispersion limit of the Korteweg de Vries equation, I, II, III*, Comm. Pure Appl. Math., 36 (1983), pp. 253–290, pp. 571–593, pp. 809–830.
- [29] G. LYNG AND P. D. MILLER, *The N -soliton of the focusing nonlinear Schrödinger equation for N large*, Comm. Pure Appl. Math., 60 (2007), pp. 951–1026.
- [30] P. D. MILLER AND S. KAMVISSIS, *On the semiclassical limit of the focusing nonlinear Schrödinger equation*, Phys. Lett. A, 247 (1998), pp. 75–86.
- [31] B. MINCHEV AND W. WRIGHT, *A review of exponential integrators for first order semi-linear problems*, Technical Report 2, The Norwegian University of Science and Technology, 2005.
- [32] J. SATSUMA AND N. YAJIMA, *Initial value problems of one-dimensional self-modulation of nonlinear waves in dispersive media*, Supp. Prog. Theo. Phys., 55 (1974), pp. 284–306.
- [33] L. F. SHAMPINE AND M. W. REICHELTL, *The MATLAB ODE suite*, SIAM J. Sci. Comput., 18 (1997), pp. 1–

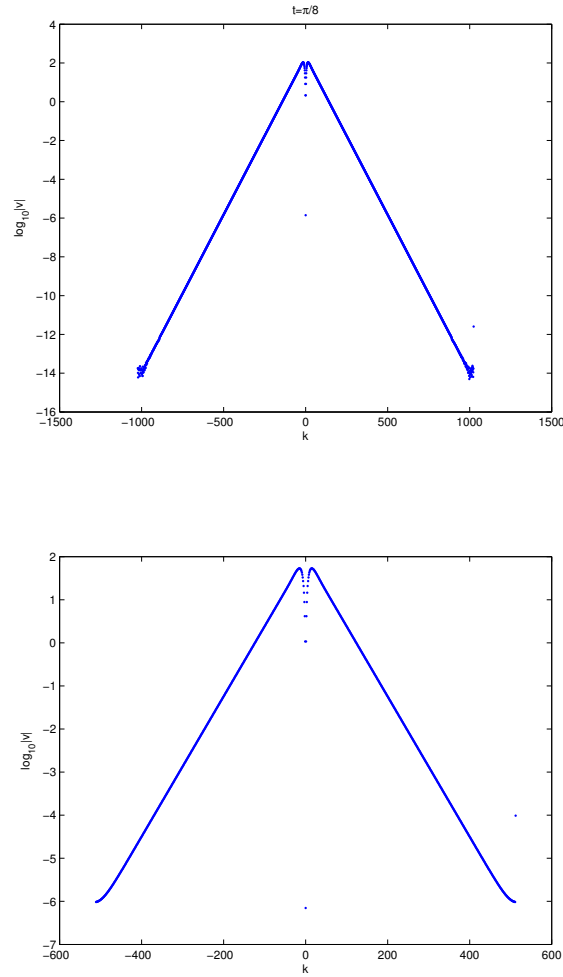


FIG. 6.3. Breather solution to the focusing NLS equation at $t = \pi/8$. The plots show the Fourier coefficients v in dependence of the spatial frequencies k for 2^{11} (top) and 2^{10} (bottom) points.

22.

- [34] L. F. SHAMPINE, M. W. REICHEL, AND J. A. KIERZENKA, *Solving index-1 DAEs in MATLAB and Simulink*, SIAM Rev., 41 (1999), pp. 538–552.
- [35] M. SCHATZMAN, *Toward non-commutative numerical analysis: High order integration in time*, J. Sci. Comput., 17 (2002), pp. 99–116.
- [36] T. SCHMELZER, PhD thesis, Oxford University, 2007.
- [37] A. TOVBIS, S. VENAKIDES, AND X. ZHOU, *On semiclassical (zero dispersion limit) solutions of the focusing nonlinear Schrödinger equation*, Comm. Pure Appl. Math., 57 (2004) pp. 877–985.
- [38] L. N. TREFETHEN, *Spectral Methods in MATLAB*, SIAM, Philadelphia, 2000.
- [39] S. VENAKIDES, *The Korteweg de Vries equations with small dispersion: higher order Lax-Levermore theory*, Comm. Pure Appl. Math., 43 (1990), pp. 335–361.
- [40] H. YOSHIDA, *Construction of higher order symplectic integrators*, Phys. Lett. A, 150 (1990), pp. 262–268.